Optical properties of calcium

C. Lopez-Rios* and C. B. Sommers†

Université de Paris XI et Centre Européen de Calcul Atomique et Moléculaire, Campus d'Orsay, Orsay, France

(Received 7 January 1974)

A detailed calculation of the energy bands, Fermi surface, density of states, $\epsilon_2(\omega)$, and photoemission energy distribution curves for an energy range of 4.2–10.6 eV has been performed on the divalent metal calcium. Over-all agreement ($\sim 5\%$) with experimental de Haas–van Alphen results was achieved using a superposition of atomic charge densities to approximate the self-consistent crystal charge density and the exchange-only local density approximation to the exchange-correlation potential. The photoemission results which included the energy distribution functions for primary and secondary electrons as well as all dipole matrix elements exhibited the empty-d-band structure above E_F. This latter result is in close agreement with the photoemission experimental measurements of Nilsson. We believe this to be the first time that the empty-d-band structure in a material has been theoretically analyzed for a photoemission process.

I. INTRODUCTION

Calcium, a face-centered-cubic alkaline-earth metal (atomic No. 20) with an atomic ground-state configuration of ($1s^2$, $2s^2$, $2p^6$, $3s^2$, $3p^6$, $4s^2$) has been the subject of many papers in the past few years.[1–11] Although an alkaline-earth metal, its behavior is more like that of a transition metal. Its d-like behavior has been verified in most band calculations which show an almost completely filled s-p band in the vicinity of the Fermi level (E_F) and five nearly empty d bands beginning at a few eV above E_F.

Due to the difficulty in achieving a single crystal, most experimental data [in particular the de Haas–Van Alphen (dHvA) Fermi-surface measurements] have been somewhat ambiguous. However, the recent photoemission results of Nilsson[12] have provided us with additional information, thus making it worthwhile to recalculate the energy bands and the photoemission properties. Using the muffin-tin and Kohn-Sham local-density exchange approximations we have been able to reproduce the Fermi surface and optical transitions to within 5% of the experimental values.

An outline of our presentation is as follows: In Sec. II, we describe the nature of the energy bands (hybridization effects) and density of states; in Sec. III, we present an estimate of the electronic specific heat; in Sec. IV, we discuss the Fermi-surface properties; and in Sec. V, we discuss the calculation of $\epsilon_2(\omega)$. Section VI is reserved for the photoemission calculation, and in Sec. VII, we present our conclusions.

II. ENERGY BANDS AND DENSITY OF STATES

Using a Korringa-Kohn-Rostoker (KKR) program developed by one of the authors[13] and an optical property program developed by Williams *et al.*,[14] we have determined the energies $E(k)$ and wave functions $T(k)$ at 89 points in $\frac{1}{48}$ of the Brillouin zone. The input parameters (aside from a lattice constant of 10.506 a.u.) were the atomic charge density for Ca and an approximation to the exchange-correlation potential $V_{xc}(\rho)$ of the form $V_{xc}(\rho) \approx V_x(\rho) \approx 2(3/\pi)^{1/3}[\rho(r)]^{1/3}$. The program was capable of calculating the bands both relativistically and nonrelativistically. The relativistic effects were calculated in order to see if the overlap of certain bands (i.e., the ratio W_2'/L_2') in the LQW direction increased. Since the Fermi level falls just above the crossing of the Q^+ and Q^- bands (~ 0.1 eV, see Fig. 1), calcium could under slight pressure (~ 50 kbar) become a semimetal. However, the existing experimental evidence[15] is inconclusive as to whether this really occurs. As can be seen (Fig. 2) and as is normally expected in the light metals, the relativistic effects are negligible (~ 0.01 eV). The amount of overlap does not change, and thus we will restrict ourselves to the results of the nonrelativistic calculation in what follows.

The energy bands (see Fig. 1) show a filled s band in the $\Gamma - \Delta - X$ direction and a nearly filled s band in the $\Gamma - W$ and $\Gamma - K$ directions. The Fermi level, at 3.8 eV above Γ_1, intersects the nearly filled bands near the points W and K, thus creating a pocket of holes in the Fermi surface (see Fig. 3). There exists a partially filled band in the z direction, which is hybridized and contains s and p components. In the Q direction, a partially filled d (Q^-) band is overlapped by an s-p (Q^+) band. The d bands which are normally occupied or partially occupied in fcc transition metals, are completely empty and have a width $[E(x_5) - E(x_1)]$ of about 5 eV.

The structure of these empty d bands can be seen in the 10-eV photon energy density plot (see Fig. 4). These are the electrons below the Fermi level which are given a large kinetic energy and are scattered by secondary processes into the

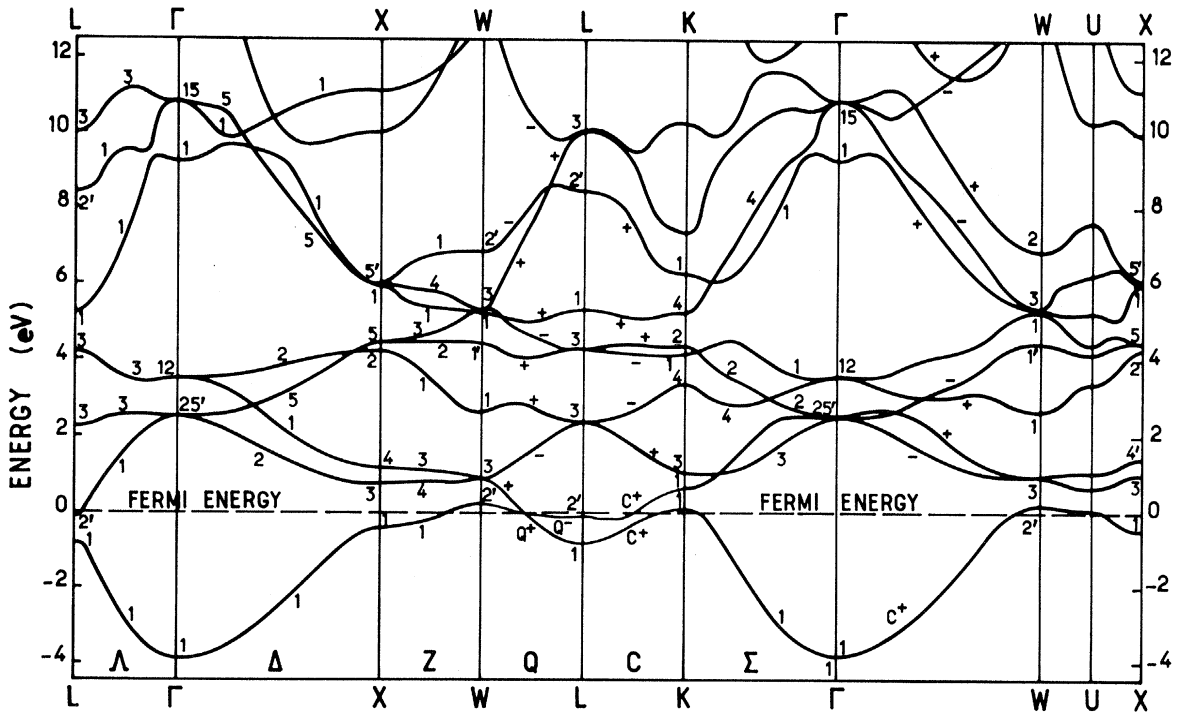

FIG. 1. Energy bands for fcc calcium.

empty d bands above E_F. This effect is elaborated on in Sec. V.

The basic nature of the bands is easily seen from the density-of-states curve $N(E)$ (see Fig. 5). The energy difference $E(W_2) - E(L_2') = 0.3$ eV shows up as a peak centered around E_F. The other principal peaks occurring at energies of 2.9, 4.1, 4.6, and 5.1 eV (No. 2–5 in Fig. 5) are easily identified. These identifications are shown in Table 1.

III. ELECTRONIC SPECIFIC HEAT

We have made an estimate of the specific heat C_v, knowing the value of $N(E_F)$, and by using a free-electron approximation $[\gamma = \pi^2 k_B^2 N(E_F)/3]$.

We have found

$$\gamma_{\text{calc}} = 1.87 \times 10^{-3}\ \text{J K}^{-2}\,(\text{g atom})^{-1}\ .$$

Using the formula

$$C_v = \gamma T + A T^3\ , \qquad (1)$$

where

$$\gamma = \gamma_0 + \gamma_1(T)$$

and

$$A = 0.16 \times 10^{-3}\ \text{J K}^{-4}\,(\text{g atom})^{-1}\ .$$

The experimental value of γ in the $0 < T < 1.8$ °K temperature range was found to be

$$\gamma_{\text{expt}} = (2.73 \pm 0.07) \times 10^{-3}\ \text{J (K)}^{-2}(\text{g atom})^{-1}.$$

The difference

$$\Delta\gamma = \gamma_{\text{expt}} - \gamma_{\text{calc}} = 0.86 \times 10^{-3}\ \text{J (K)}^{-2}(\text{g atom})^{-1}$$

was attributed to electron-phonon effects.

The contribution to $\gamma_1(T)$ by the electron-phonon interaction for Ca can be shown (see Ref. 16) to be of the same order of magnitude as γ_0[i.e., $\gamma_1(T)/\gamma_0 \sim 1$] in the $0 < T < 4$ °K temperature range, and thus qualitatively accounts for the difference of 0.86×10^{-3} J (K)$^{-2}$(g atom)$^{-1}$.

IV. FERMI SURFACE

Figure 3 shows a three-dimensional plot of the first-zone orbits as determined from our calculation. The corresponding cross-sectional areas are shown in Figs. 6(a), 6(b), and 6(c) for both the

TABLE I. Principal band contributions to the peaks in the density of states.

Peak energy (eV)	Principal band contributing
2.9	Q^+ between L_3 and W_1
4.1	Q^+ between L_3 and W_1' C^- between L_3 and K_1
4.6	Z_2 between W_1' and X_5 C^+ between L_3 and K_2
5.1	C^+ between L_1' and K_4 Q^+ between L_1 and W_1

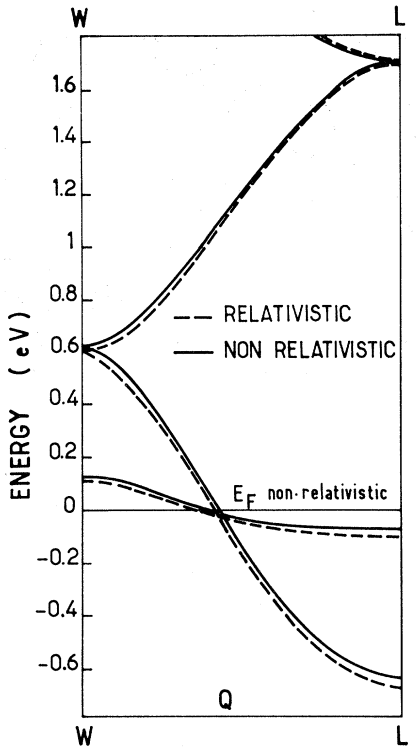

FIG. 2. Comparison of relativistic and nonrelativistic energy bands in the WQL direction.

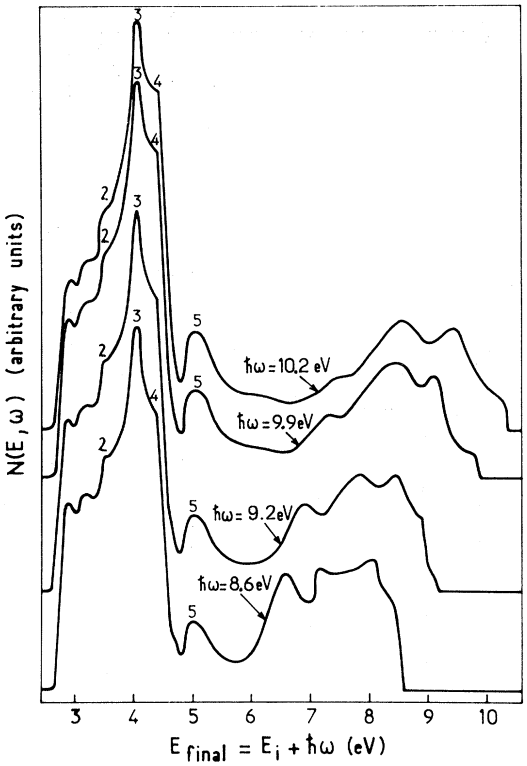

FIG. 4. Photoemitted density of electrons for the energy range 8.6–10.2 eV.

first and the second zone. The notation we use is that of Harrison[2] (Latin letters) and Condon and Marcus[17] (Greek letters). Our results will be compared with the experiments of Condon and Marcus (CM) and Jenkins and Datars[18] (JD). It should also be noted that the samples of JD were high-purity single crystals, while those of CM were polycrystalline.

In the first zone (Fig. 3), we have found a neck orbit of holes (a), which is centered at K (or U) in the (110) plane [see Fig. 6(b)]. This orbit (a) is extremely sensitive to the position of the Fermi level which is situated only 0.15 eV above $E(L_2')$ (see Fig. 1). The period of this orbit $P_a = 3.18 \times 10^{-7}$ G^{-1} is within 4% of the experimental value of JD ($P_{expt} = 3.08 \times 10^{-7}$ G^{-1}).

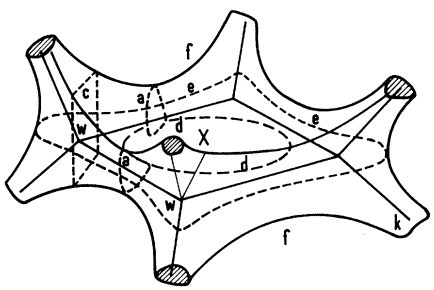

FIG. 3. Three dimensional plot of Fermi surface orbits in the first Brillouin zone.

In the (100) plane, we have two hole orbits centered at X on the square face, d, which is nearly circular with a period $P_d = 0.205 \times 10^{-7}$ G^{-1}, and e, with a period $P_e = 0.094 \times 10^{-7}$ G^{-1} [see Figs. 6(a) and 6(c)]. These two orbits have been predicted by other calculations,[7,10] but have not been verified experimentally. JD claim that the reason for not being able to detect the orbit d is due to its limited angular range. The curvature factor $|\partial A_H/\partial k_H|^{-1/2}$ dominates the dHvA amplitude and is thus difficult to detect, while the reason for not being able to find orbit e was attributed to the impurities in the sample.

The orbit c, centered about W, in a plane perpendicular to the [100] direction (Fig. 3), with a period $P_c = (0.79 \pm 0.09) \times 10^{-7}$ G^{-1} agrees with the experimental value of JD (0.75×10^{-7} G^{-1}).

On the hexagonal face [Fig. 6(a)], we have a circular orbit of electrons (f), centered at L, with a period $P_f = 0.116 \times 10^{-7}$ G^{-1}. The radius of this orbit (0.54 Å^{-1}) is comparable with that of the equivalent free-electron orbit (0.52 Å^{-1}).

The orbit a, which connects the orbits d, e, and

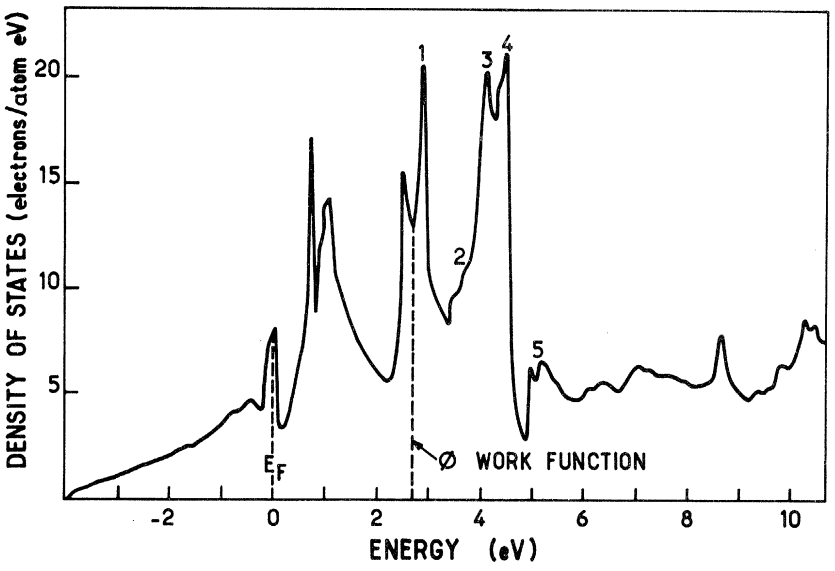

FIG. 5. Density of states.

f, and the orbit c, which connects the orbits e and f, give rise to a Fermi surface, in the first zone, which *is completely connected.*

In the second zone, we have found a hole pocket centered at L, taking the form of an ellipse in the (110) plane (orbit b), with a period $P_b = (0.66 \pm 0.10) \times 10^{-7}\ \mathrm{G}^{-1}$. This orbit is extremely difficult to calculate as a change in E_F of 0.07 eV is enough to make the orbit disappear. It is for this reason that the calculated error in P_b is of the order of 15%. The experimental value is $0.58 \times 10^{-7}\ \mathrm{G}^{-1}$.

On the hexagonal face [(111) plane], we obtain a circular orbit (g) of period $P_g = 0.149 \times 10^{-7}\ \mathrm{G}^{-1}$. This orbit has not as yet been detected experimentally, but has been predicted by all previous calculations.

A summary of our results is shown in Table II.

V. $\epsilon_2(\omega)$

The interband contribution to the imaginary part of the dielectric constant is defined as

$$\epsilon_2(\omega) = \frac{1}{\omega^2} \sum_{n,n'} \int d^3k\, f_n(1 - f_{n'}) \left| \langle nk | \vec{p} | n'k \rangle \right|^2 \times \delta(E_n(k) - E_{n'}(k) - \hbar\omega)\ , \qquad (2)$$

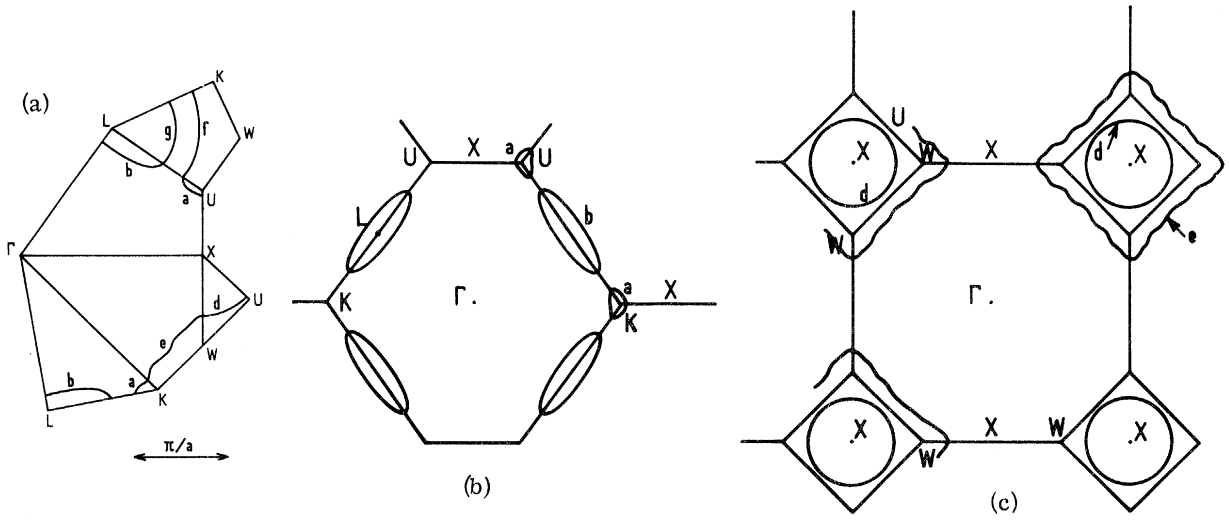

FIG. 6. (a) Cross-sectional mapping of de Haas–van Alphen orbits of the first and second zones. The connectivity of the first zone orbits is seen by following the paths a-e-d and a-f. (b) and (c) Over-all cross-sectional view of various Fermi-surface orbits.

TABLE II. Comparison of various calculations with the experimental dHvA orbits. The effective mass m_c/m_0 is given when possible.

		Period (10^{-7} G^{-1})					m_c/m_0	
Orbit	Direction	APW (Ref. 7)	Cellular (Ref. 10)	Our results KKR	CM (Ref. 17)	JD (Ref. 18)	KKR	JD (Ref. 18)
d	[100]	0.228	0.198	0.205				
e	[100]	0.095	0.085	0.094				
c or α	[100]	0.61		0.79 ∓ 0.09	0.77 ∓ 0.04	0.78	0.66	0.60 ∓ 0.03
a or γ	[110]	8.12	3.65	3.18 ∓ 0.36	3.05 ∓ 0.06	3.08		
f	[111]			0.116				
b or β	[110]	0.49		0.66 ∓ 0.10	0.57 0.03	0.58	0.54	0.52 ∓ 0.02
g	[111]	0.178	0.14	0.149				
δ	[110]					0.79		

where f_n is the Fermi function and $E_n(k)$ and $E_{n'}(k)$ are the initial (filled) and final (empty) states, respectively. The matrix elements $\langle nk|\vec{p}|n'k\rangle$ have been included in the calculation and have not been taken as a constant independent of k. In Fig. 7, we present the results of such a calculation for a range of photon frequencies $2 \leq \hbar\omega \leq 9$ eV. We were able to determine the major contributions to the peaks in $\epsilon_2(\omega)$ as coming from regions in k space centered about a certain k_0 and due to certain band transitions. These values appear above the three major peaks of Fig. 7.

In Fig. 8, we have plotted the separate band-pair contributions. The strongest contributions come from the 1-4 and 1-6 band pairs (band 1 being a hybridized sp band). The transitions starting from band 2 (d-like band) contribute less because of the $\Delta l = \pm 1$ selection rule.

The largest peak centered about 5 eV is due to the d bands falling between 4 and 6 eV above the Fermi level and being nearly flat throughout the zone.

In Table III, we have listed the optical transitions as well as the coordinates (in k space) of the volume element giving the largest contribution along with its variance. It is regretable that there are no experiments to date on $\epsilon_2(\omega)$ in the optical region of interest. However, we have used these calculations in interpreting the photoemission results.

VI. PHOTOEMISSION

The photoemitted energy distribution, including those electrons once scattered, can be written (see Ref. 14) as

$$N(E,\omega) = T_F(1-T_f)\left(\tilde{D}'(E,\omega) + \int_E^{\hbar\omega+E_F} S_{ee}(E',E)\tilde{D}'(E',\omega)\,dE'\right), \quad (3)$$

where

$$T_F = \frac{1}{2}\left[1 - \left(\frac{\phi - E_F}{E - E_F}\right)^{1/2}\right], \qquad E > \phi$$

and

$$D'(E,\omega) = \left(\int_{E_F}^{\infty} D(E',\omega)\,dE'\right)^{-1} \sum_{n,n'} \int d^3k\, f_n(1-f_{n'}) \times |\langle nk|\vec{p}|n'k\rangle|^2 \delta(E - E_{n'}(k)) \times \delta(E - \hbar\omega - E_n(k))\, T(k,E,\omega)\,. \quad (4)$$

$\tilde{D}'(E,\omega)$ is the energy distribution $D(E,\omega)$ which has been convolved with lifetime-broadening Lorentzians to account for many-electrons effects. The second term in Eq. (3) accounts for the secondary electrons due to pair-creation interactions.

There are two ranges of photon frequencies of interest (i.e., experimental results available), that of 8–11 eV by Nilsson, and of 4–5 eV by Kress and Lapeyre[19] (KL). We will discuss each range separately in what follows.

A. $\hbar\omega$=8-10 eV

Let us look first at the curves of Fig. 4. Here we have plotted $N(E,\omega)$ vs the final-state energies $E_{\text{final}} = E_{\text{initial}} - \hbar\omega$. We immediately notice that in the energy range 3–5 eV, the principal peaks in $N(E,\omega)$ (peaks 2–5) do not change as a function of

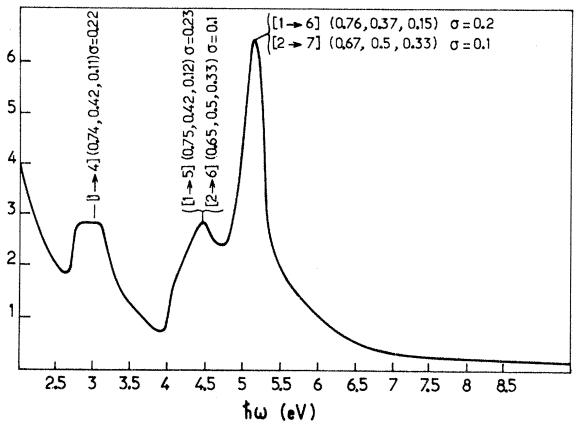

FIG. 7. Imaginary part of dielectric constant $\epsilon_2(\omega)$.

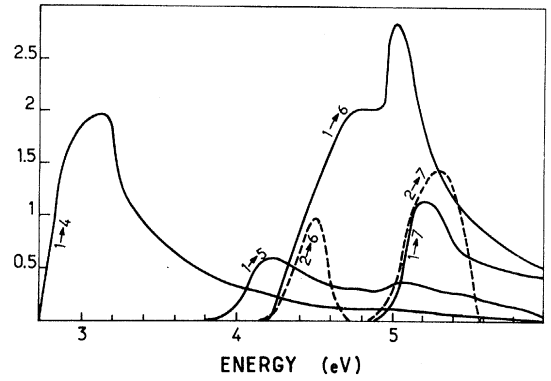

FIG. 8. Band-pair contributions to $\epsilon_2(\omega)$.

energy. This implies that the nondirect transition model[20] can be used to explain our results. In fact, what we see from our calculation is that electrons just below or near E_F are displaced by secondary scattering and have scattered into the empty d bands above E_F. The first term in Eq. (3) describing the direct transitions is weak compared to the second describing once-scattered electrons. The nondirect model predicts an energy distribution

TABLE III. Band-pair contributions to $\epsilon_2(\omega)$.

$\hbar\omega$ (eV)	Band	k-space locations in units of $2\pi/a$	Variance σ
3.400	1	(0.708, 0.346, 0.119)	0.224
	2	no contributions	•••
3.536	1	(0.690, 0.337, 0.119)	0.223
	2	no contributions	•••
3.808	1	(0.649, 0.311, 0.113)	0.223
	2	(0.775, 0.500, 0.225)	0.025
3.944	1	(0.633, 0.305, 0.109)	0.274
	2	(0.734, 0.511, 0.240)	0.081
4.080	1	(0.695, 0.373, 0.135)	0.236
	2	(0.697, 0.508, 0.270)	0.095
4.216	1	(0.710, 0.403, 0.134)	0.233
	2	(0.634, 0.495, 0.334)	0.116
4.357	1	(0.735, 0.437, 0.137)	0.257
	2	(0.598, 0.489, 0.389)	0.088
4.488	1	(0.747, 0.467, 0.120)	0.230
	2	(0.650, 0.504, 0.330)	0.100
4.624	1	(0.747, 0.469, 0.116)	0.206
	2	(0.743, 0.480, 0.274)	0.106
4.760	1	(0.736, 0.470, 0.123)	0.191
	2	(0.767, 0.480, 0.249)	0.077
4.896	1	(0.734, 0.448, 0.125)	0.185
	2	(0.774, 0.500, 0.226)	0.037
5.032	1	(0.771, 0.391, 0.118)	0.197
	2	(0.746, 0.495, 0.258)	0.059
5.168	1	(0.763, 0.371, 0.147)	0.195
	2	(0.670, 0.507, 0.292)	0.094
5.304	1	(0.720, 0.387, 0.153)	0.198
	2	(0.613, 0.486, 0.368)	0.095
5.440	1	(0.681, 0.369, 0.150)	0.197
	2	(0.636, 0.433, 0.402)	0.038

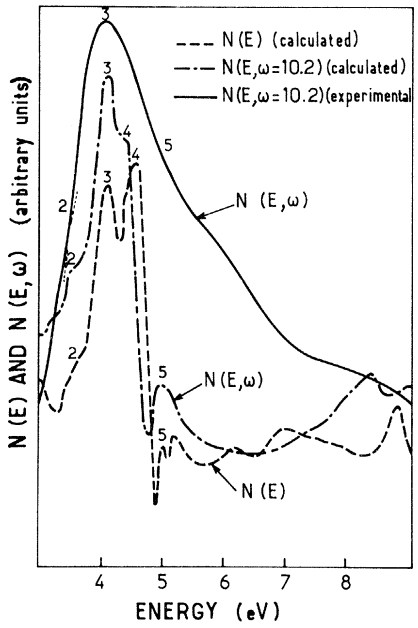

FIG. 9. Comparison of the density of states $N(E)$ with the photoemitted density of electrons $N(E,\omega)$ as calculated and measured experimentally for $\hbar\omega = 10.2$ eV.

$$N(E,\omega) \sim C\rho_v(E-\hbar\omega)\rho_c(E)\ . \tag{5}$$

In Ca, ρ_v is structureless except around E_F, whereas $\rho_c(E)$ contains almost all of the structure (see Fig. 3) which appears in $N(E,\omega)$. This is in

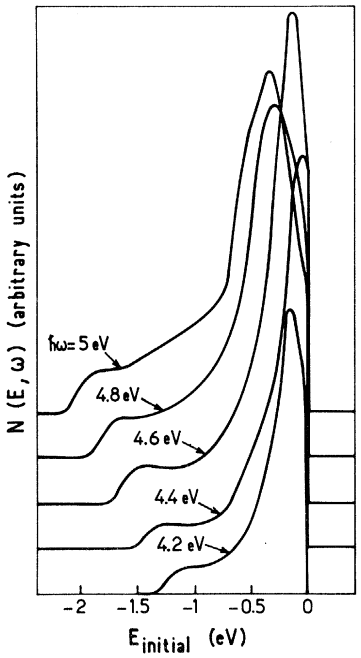

FIG. 10. Photoemitted density of electrons $N(E,\omega)$ calculated for the 4.2–5-eV photon energies.

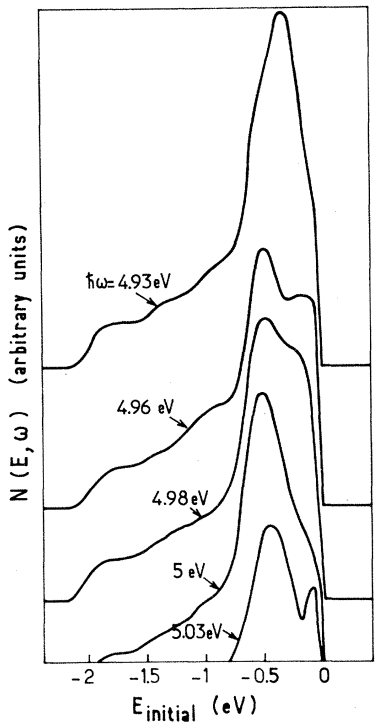

FIG. 11. Photoemitted density of electrons $N(E,\omega)$ calculated for the 4.93–5.03-eV photon energies.

contrast to metals usually studied. In order to see this more clearly, we have superimposed (see Fig. 9) the density of states $N(E)$ and $N(E,\omega)$ calculated for $\omega=10.2$ eV as well as $N_{\text{expt}}(E,\omega=10.2)$ obtained by Nilsson. Comparing the theoretical curves we see that they are nearly identical, showing peaks (2, 3, 4, 5) which agree in energy as well as relative magnitude.

If we now look at the experimental results for the same photon energy, we see a close resemblance. The major peak (3) at 4.1 eV lines up with our peak (3) at 4.1 eV. The detailed structure however is missing but is indicated by a change in slope at points (2) and (5) in $N_{\text{expt}}(E,\omega)$ occurring at energies 3.6 and 5.0 eV, respectively. Moreover, the fact that peak (3) at 4.1 eV coincides with our calculation shows that the choice of the exchange-correlation potential used (Kohn-Sham) is correct. Had we used a Slater-type exchange with $\alpha\neq\frac{2}{3}$, the peak (3) which is due to the empty-d-band structure above E_F would not be centered at 4.1 eV.

B. $\hbar\omega$=4–5 eV

In this range of photon energies there are considerable changes in structure when we look at $N(E,\omega)$ as a function of ω. This then would tend to support a direct transition model explanation. In Fig. 10, we show the 4–5-eV range and in Fig. 11, we plot $N(E,\omega)$ on an expanded scale (4.93–5.03 eV).

The large peak starting at about 4.2 eV is in agreement with the onset of the (1–6) and somewhat smaller (2–7) optical transitions (see Fig. 8) at this energy. Again, at about 4.9 eV, another strong peak emerges (see Fig. 11) and this is attributed to the onset and strong peaking of the (1–6) band-pair contribution to $\epsilon_2(\omega)$ at the same energy. We also attribute a small peak in $N(E,\omega)$ for $\hbar\omega=5.03$ eV as due to the shoulders in the (1–7) and (2–7) band-pairs. The experimental results of KL show none of this structure at these energies. Moreover, at 8 eV their results differ markably from those of Nilsson (at 8 eV), which we tend to believe because of the results of our analysis in Sec. VI A.

VII. CONCLUSIONS

The aim of this work has been to calculate as many of the one-electron properties as possible in a metal, in an *ab initio* sense. After making two approximations, namely that of the muffin-tin potential, and secondly that of replacing the exchange-correlation operator by a local density operator, we were able to arrive at a model for calcium which reasonably explained the experimental results. No attempt was made to take into account such many-body effects as the energy dependence of the self-energy and vertex corrections, which play an important role in the photoemission process. These effects however, are more important when dealing with transitions emanating from localized states or bands. This is not the case for calcium, as the d bands lie above the Fermi level. There are however several questions to be resolved in terms of the photoemission results. Our calculation predicts a peak at 4.1 eV in the $N(E,\hbar\omega)$ spectrum at high photon energies. We have in an approximate way [see Eq. (4)] taken into account the effects of the work function cutoff and the secondary electron distribution which normally give rise to such a peak in the experimental situation. We would therefore suggest a more detailed experiment, especially at high photon energies in order to see if this peak remains (does not appreciably broaden), and thus verify its d-band origin. Secondly, a more detailed experiment in the 4–5 eV range is suggested in order to see if our predicted structure exists. This plus a measurement of $\epsilon_2(\omega)$ we feel would tie all the optical properties together in a coherent manner.

Lastly, we wish to stress the importance of using the density of states and the band-pair optical transitions in interpreting the photoemission results.

The authors wish to thank Dr. A. Williams for making available several computer programs and for valuable discussions in helping to interpret the photoemission results.

*Present address. Commissariat A L'Energie Atomique C. E. L, B. P. 27, 94190 Villeneuve St. Georges, France.

†Present address. Physique des Solides Bât. 510 Campus d'Orsay, 91 Orsay, France.

[1]M. F. Manning and H. M. Krutter, Phys. Rev. 51, 761 (1937).

[2]W. A. Harrison, Phys. Rev. 131, 2433 (1963).

[3]S. L. Altmann and A. P. Cracknell, Proc. Phys. Soc. Lond. 84, 761 (1964).

[4](a) B. Vasari and V. Heine, Philos. Mag. 15, 731 (1967); (b) B. Vasari, A. O. E. Animalu, and V. Heine, Phys. Rev. 154, 535 (1967); (c) B. Vasari, Rev. Mod. Phys. 40, 776 (1968).

[5]S. L. Altmann, R. C. Harford, and R. G. Blake, J. Phys. F. 1, 791 (1971).

[6]J. A. Dreesen and L. Pyensen, Phys. Rev. B 2, 4852 (1970).

[7]J. M. McCaffrey, J. R. Anderson, and D. A. Papaconstantopoulos, Phys. Rev. B 7, 674 (1973).

[8]S. Chatterjee and P. J. Chakraborti, J. Phys. F 1, 638 (1971).

[9]M. Ross and K. Johnson, J. Phys. F. 13 (1971).

[10]S. L. Altmann, R. C. Harford, and R. G. Blake, J. Phys. F. 2, 1062 (1972).

[11]R. W. Williams and H. L. Davis, Nat. Bur. Stds. p. 34 (1969).

[12]P. O. Nilsson, G. Arbman, D. E. Eastman, Solid State Commun. 12, 627 (1973).

[13]C. B. Sommers and H. Amar, Phys. Rev. 188, 1117 (1969).

[14]A. R. Williams, Nat. Bur. Stds. Spec. Publ. 323 (1970).

[15]H. G. Drickamer, Solid State Phys. 17 (1965).

[16]G. Grimvall, J. Phys. Chem. Solids 29, 1221 (1968).

[17]J. H. Condon and J. A. Marcus, Phys. Rev. 134, 446 (1964).

[18]R. M. Jenkins and W. R. Datars, Phys. Rev. B 7, 2269 (1973).

[19]K. A. Kress and G. J. Lapeyre, Solid State Commun. 9, 827 (1971).

[20]C. N. Berglund and W. E. Spicer, Phys. Rev. 4, A136 (1964).